12th International Symposium on Turbulence and Shear Flow Phenomena (TSFP12)
Osaka, Japan (Online), July 19–22, 2022

NEAR-FIELD TURBULENCE IN A MULTI-FAN WIND TUNNEL

Jovan Nedić and Austin L'Ecuyer
Department of Mechanical Engineering
McGill University
817 Sherbrooke Street West, Montréal, Québec H3A 0C3, Canada
jovan.nedic@mcgill.ca

ABSTRACT

We examine turbulence generated by a multi-fan wind tunnel, comprised of a 9x9 grid of small fans which can be individually controlled. A checkerboard pattern is considered, where the fans are alternatively set to one of two different velocities. It is shown that the turbulence intensity and integral length scale can be increased by increasing the shear ratio, defined as the ratio between the higher and lower velocities given to the fans. Moreover, the turbulence generated by the multi-fan wind tunnel has strong similarities to decaying grid-turbulence, exhibiting a region of faster decaying turbulence closer to the fans. This region was also found to exhibit non-equilibrium properties, namely one where the dissipation parameter was not constant.

INTRODUCTION

A variety of different methods have been employed in the past to generate decaying homogeneous and isotropic turbulence. The most classical approach has been the use of passive grids, which are comprised of an array of regularly spaced perpendicular bars with a thickness d, to create a mesh with a spacing of M. A vast body of work has utilised these grids to examine the fundamental theories of turbulence. The Taylor-based Reynolds number they create, however, has typically been confined to $\mathrm{Re}_\lambda < 150$, which decreases with increasing downstream distance from the grid. In order to increase the range of possible Re_λ, Makita (1991) developed an "active grid" comprised of rectangular bars or rods with an array of triangular agitator wings on bars attached to motors; the bars and agitator wings spin, which is the active part of the grid. The bars randomly change direction and rotation speed which creates the highest turbulent kinetic energy and integral length scale. Over the years, through various design tweaks and modifications to the algorithms used to actuate the motors (Mydlarski, 2017), have resulted in large Re_λ, in some cases as high as $\mathrm{Re}_\lambda = 1100$ (Larssen & Devenport, 2011).

A recent advancement in wind tunnel turbulence generation has been the use of multi-fan wind tunnels (MFWT), whereby the turbulence is generated by an array of small fans arranged in a planar grid, ideally with each fan being controlled separately. Originally designed to generate atmospheric boundary layers (Nishi *et al.*, 1999), recent efforts have examined ways in which the turbulence can be controlled via dynamic modulation of all of the fans (Ozono *et al.*, 2006; Ozono & Ikeda, 2018; Takamure & Ozono, 2019), again with the objective of recreating atmospheric conditions. The region where such properties of the flow were considered are notably far from the fans themselves, often more than 30 fans dimensions away. What is still unknown, however, is how the turbulence evolves in the region closer to the fans.

One of the major attractions for using MFWT for generating turbulence is that it affords the user with increased control over the flow patterns they can create. For example, by alternating the speed between adjacent fans in a checkerboard pattern, one can, in theory, replicate the conditions of a passive grid. Moreover, it is possible to examine the effects of initial shear on the turbulence statistics, by changing the ratio of two velocities given by the fans. Therefore, a shear parameter

$$S_r = U_2/U_1 \tag{1}$$

can be defined, where U_2 is the higher of the two velocities i.e., $U_2 \geq U_1$. This implies that $1 \leq S_r \leq \infty$, where the upper limit corresponds to the case of $U_1 = 0$ m/s. The objective of this study is to investigate the near-field of MFWT-generated turbulence for such a flow pattern, and determine to what extent the turbulence is similar, or dissimilar, to turbulence generated by passive grids. A hypothesis that we would also like to examine is whether increasing the shear ratio of the fans will lead to increased turbulence levels and integral scales.

EXPERIMENTAL FACILITY

A new multi-fan wind tunnel (MFWT) was constructed for the purpose of this study. A total of $N = 81$ fans were used to create a 9-by-9 2D planar grid, as shown in fig. 1; the grid of fans is referred to as the *fan wall*. Each fan unit was $F = 80$ mm in width and height, and pushed fluid through an opening with an outer diameter of $D_o = 78$ mm and an inner diameter of $D_i = 36$ mm. The motors, located within the centre of the fan unit, was driven by a pulse-width modulated (PWM) signal, provided by a *National Instruments* NI PCIe-6341 multifunction I/O (input/output) device connected to a BNC-2110 connector block. Currently, only four unique PWMs can be sent to the fans. The grid of fans are secured by a structure made of 3 mm thick medium density fiberboard (MDF); this resulted in the square test section having a height and width of 750 mm-by-750 mm i.e. $W = 750$ mm, as shown in fig. 1. The subsequent fan spacing, from centre-to-centre, is hence $M = 83$ mm. Given the open area through which fluid is pushed by each fan, and the total cross-sectional area of the facility, one can calculate an open area ratio as

$$OAR = \frac{\pi N(D_o^2 - D_i^2)}{4W^2}\,, \tag{2}$$

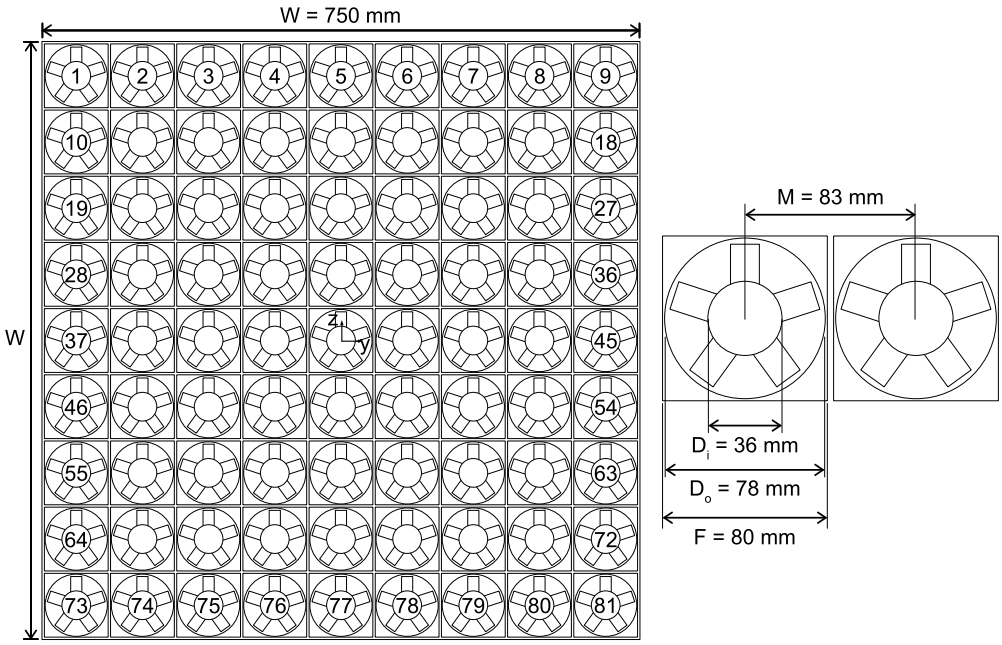

Figure 1. Dimensions, and arrangement, of the fans used to create the turbulent flow field in the multi-fan wind tunnel. Note that the co-ordinate system is centred in the middle of fan 41.

which for this facility is 0.54. Its function is to act as a corollary to solidity ratio of passive grids. A test section of length 2.4 m was attached to the fan wall, with a traversing mechanism that allowed for measurements in the streamwise x and planar y,z directions; the co-ordinate system originated at the centre of the middle fan i.e., fan 41 in fig. 1. The final assembly allowed for measurements over approximate non-dimensional distances of $4 \leq x/M \leq 22$, $-1.5 \leq y/M \leq 1.5$, and $-2 \leq z/M \leq 2$. Measurements of the instantaneous streamwise u and transverse v velocity were obtained using a *Dantec* X-wire sensor, driven by a *Dantec Streamline* constant temperature anemometer. Data was sampled at a rate of 75 kHz for 60 seconds, which was sufficient to capture converged statistics, and low-pass filtered (analogue) at 30 kHz. An iterative method was then used in the post-processing to find the Kolmogorov frequency, with a fourth-order low-pass Butterworth filter applied digitally to the data at 1.3 times the Kolmorogorv frequency. Additional post-processing of the cross-wire data was implemented following the procedure by Burattini (2008) to account for wire separation effects on velocity derivatives.

RESULTS

Mean flow properties

A calibration was first conducted to relate the PWM signal sent to the fans to their output flow velocity. Based on these measurements, the operating range of the fans was found to be 1.5 m/s $\leq U_f \leq$ 7.9 m/s. In order to investigate the widest possible range of shear ratios, the bulk freestream velocity was set to $U_\infty = 5$ m/s, which would allow for shear ratios of $1 \leq S_r \leq 3.5$. Note that $S_r = 1$ is equivalent to having all the fans operating at the same velocity, whilst shear ratios of $S_r > 1$ had the even-numbered fans operating at the same velocity U_2, which was higher than the velocity U_1 from the odd-numbered fans – see fig. 1 for fan numbering system.

The streamwise development of the normalised streamwise velocity, along the centreline of the tunnel $(x,0,0)$, is shown in fig. 2 for $S_r = 1$, 1.5, 2, 2.5, 3, and 3.5. For $x > 13M$, the mean flow is approximately constant for all shear ratios;

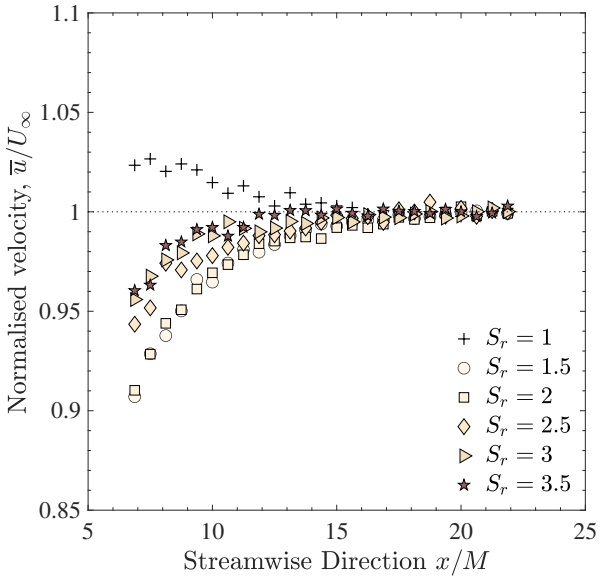

Figure 2. Streamwise development of the centreline mean velocity for various shear ratios.

this is also the downstream location where the planar measurements (not shown here for brevity) indicate that the mean flow is also approximately uniform. For $x < 13M$, there is a clear dependence on shear ratio where, somewhat surprisingly, the larger shear ratios approach $\overline{u} = U_\infty$ faster. Note here that $\overline{u}$ is the mean streamwise velocity.

Although such a flow pattern is hypothesised to replicate the conditions of a passive grid, it is important to stress some of the key differences between the two in the manner in which turbulence is generated. For a passive grid, an incoming uniform mean flow is pushed through the grid, where wake-like regions are created behind the bars of the grid, and jet-like regions are created in the space between the bars, with resulting

shear produces the turbulence. By changing the solidity ratio of the grid (solid area of bars to cross section of the tunnel), the relative dominance of the wake-like vs. jet-like regions is altered. For a MFWT, no such regions of wake-like flow exist, since the flow is pushed out by the fans in the form of a jet, which merge at some distance upstream of the fan. In addition to this, the rotation of the fans can lead to the creation of a mean rotation in the flow, at least in the vicinity of the fans. Nevertheless, the fundamental principal for turbulence generation remains the same between the two facilities, that being the creation of a velocity shear.

Centreline turbulence statistics

Examining the streamwise large-scale isotropy, fig. 3, we note that $u_{rms}/v_{rms} \approx 1$ to within 5%, where u_{rms} is the root mean square of the streamwise velocity component. Such values of large-scale isotropy are comparable to the measurements from grid-generated turbulence, particularly those where a secondary contraction was used to specifically improve isotropy (Comte-Bellot & Corrsin, 1966; Hearst & Lavoie, 2016). The nature of the small-scale isotropy is left for a future study, as the primary objective of this study is a focus on the large-scale turbulence properties generated by the fans. Homogeneity of the turbulent field was determined by investigating the spanwise and transverse variation of both u_{rms} and v_{rms}. For $x > 13M$, the ratio of these values to their corresponding value on the centreline was found to be constant to within $\pm 5\%$, which is again inline with previous measurements on grid-generated turbulence. Given this, the remainder of the turbulence statistics are presented along the centreline only i.e., along $(x,0,0)$. It is also worth noting that the observed large-scale isotropy for this facility is better than what was obtained by Ozono & Ikeda (2018), who had $u_{rms} \approx 1.1 v_{rms}$, and this at a much further downstream distance from the fans, whose facility also included a honeycomb.

By assuming that the spanwise velocity component w (along the z direction) is the same as the transverse velocity component, we may write the total turbulent kinetic energy as $k = 0.5(\overline{u'^2} + 2\overline{v'^2})$, where primes denote fluctuating values (mean subtracted values) of the velocity signal, and the overline denotes an average. Figure 4a shows the normalised kinetic energy for a range of shear ratios, where it is evident that the kinetic energy is decaying with streamwise distance, as is the case for both passive grids and active grids. Furthermore, we note that increasing the shear ratio increases the turbulent kinetic energy of the flow. For example, at the closest measurement location of $x = 7M$, the turbulent kinetic energy increased by almost 50% when increasing the shear ratio from $S_r = 1$ to $S_r = 3.5$.

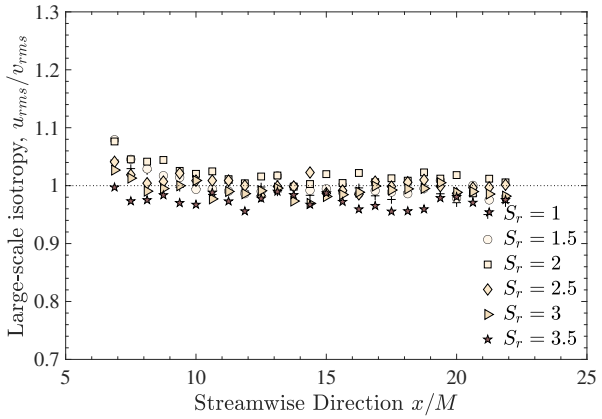

Figure 3. Large-scale isotropy along the centreline for various shear ratios.

Table 1. Virtual origin x_0/M and the decay exponent m in the near-field and ($x < 13M$) and far-field, shown as bold numbers in brackets.

S_r	x_o/M	m
1.0	-1.44 (**6.49**)	2.00 (**1.06**)
1.5	-0.98 (**3.13**)	2.23 (**1.58**)
2.0	0.27 (**2.71**)	1.90 (**1.54**)
2.5	0.49 (**3.19**)	1.92 (**1.45**)
3.0	-1.48 (**2.47**)	2.30 (**1.52**)
3.5	-1.58 (**5.80**)	2.33 (**1.17**)

As with decaying grid-generated turbulence, we fit the turbulent kinetic energy with the power law of the form

$$\frac{k}{U_\infty^2} = A\left(\frac{x - x_0}{M}\right)^{-m}, \tag{3}$$

where m is the decay exponent, x_0 is a virtual origin for the power-law fit, and A is a scaling constant. It is plausible, indeed likely, that all three variables on the right hand side of eq. (3) are functions of the shear ratio, and is an aspect that shall be investigated further in a future study. Research over the last two decades has indicated that decaying grid-generated turbulence in the vicinity of the grid exhibits two regions with distinct decay rates of the turbulent kinetic energy (Valente & Vassilicos, 2011; Hearst & Lavoie, 2016; Nedić & Tavoularis, 2016*b*). To identify if such regions exist in this flow, and extract the corresponding decay rates, the algorithm proposed by Valente & Vassilicos (2011) is used. Two distinct regions, as indicated by a noticeable change in the decay exponent m, were identified; one in the near-field $x < 13M$ another in the far-field $x \geq 13M$. The decay exponent, and the virtual origin, for each of the shear flows, are presented in table 1. Based on these results, it does not appear that the virtual origin, or the decay exponent, are a function of the shear ratio. Nevertheless, there is a clear difference in both the virtual origin and decay exponent in the two identified regions, most notable of which is that the decay exponent is higher in the near-field as compared to the far-field. Fits of eq. (3), using the values shown in table 1, are shown in fig. 4a for both regions. If we assume that the shear ratio has no discernible influence on the virtual origin and decay exponents, one can therefore determine the average decay exponent in the near-field, $x < 13M$, as $m_{near} = 2.11$, and in the far-field as $m_{far} = 1.39$. These values are similar to those seen in the near- and far-field of both regular and fractal grids (e.g., Nedić & Tavoularis, 2016*b*).

The streamwise variation of the streamwise integral length scale $L_{11,1}$ is shown in fig. 4b, which was calculated by integrating the autocorrelation function to is first zero crossing. Generally, the integral scale increases with streamwise distance, but remains, for all shear ratios, smaller than the fan size, as well as smaller than the spacing between the fans. Ozono & Ikeda (2018) similarly observed that the integral scale was smaller than the fan size, but noted that it tended towards it far downstream; by $x \approx 60M$, $L_{11,1} \approx 0.93M$. By

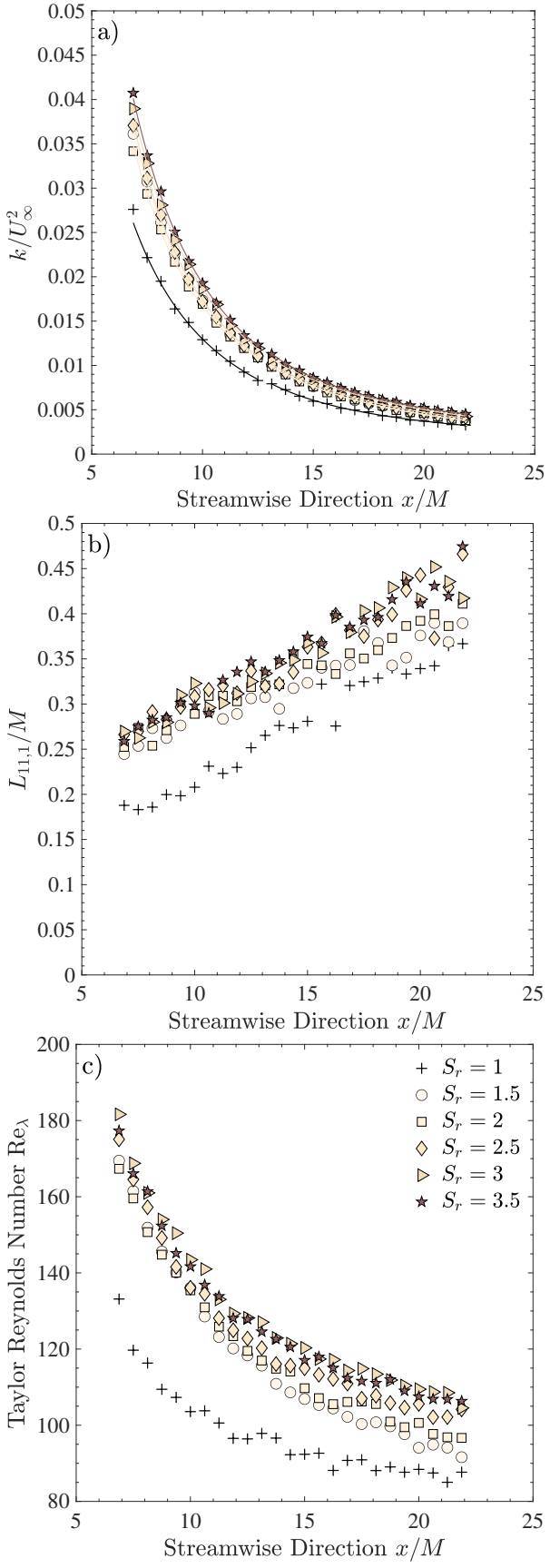

Figure 4. a) Decay of turbulent kinetic energy, b) growth of integral scale , and c) variation of Taylor Reynolds number with streamwise distance for various shear ratios.

increasing the shear ratio one is able to increase the integral length scale, in some cases by as much as 45%. This is to be expected, since the turbulent kinetic energy is a function of the shear ratio, whereas the decay exponent, for both regions, is independent of shear ratio.

Streamwise variation of the Taylor Reynolds number, defined as $\mathrm{Re}_\lambda = \lambda u_{rms}/\nu$, along the centreline is presented in fig. 4c. Note that the Taylor microscale was estimated as $\lambda = u_{rms}\sqrt{15\nu/\varepsilon}$, using the x-wire estimate for the dissipation rate $\varepsilon = 3\nu[\overline{(\partial u/\partial x)^2} + 2\overline{(\partial v/\partial x)^2}]$. Over the entire measurement region, the Taylor Reynolds number for the $S_r = 1$ case (all fans on at same speed) ranged from $\mathrm{Re}_\lambda = 140$ at the closest location, reaching a value of $\mathrm{Re}_\lambda = 85$ at $x = 22M$. This range of Reynolds numbers is again comparable with passive grids with equivalent mesh spacing; see, for example, the RG80 (mesh spacing = 80 mm) results of Nedić & Tavoularis (2016*b*). Increasing the shear ratio produced a noticeable increase in Re_λ, as much as 40% in some cases. Given the increase in both the kinetic energy and integral scale, the increase in Taylor Reynolds number is to be expected.

It is worth mentioning that examination of the energy spectra (not shown here) indicated a clear inertial sub-range, whose slope was close to -5/3, for all shear ratios and downstream locations. As expected, it was observed that the width of the inertial sub-range increased with increasing Re_λ.

For all turbulence properties presented here, a very clear increase in all parameters was observed as the shear ratio is increased from $S_r = 1$. This therefore suggests that control of the turbulence parameters is, to some degree, possible by simply varying the shear ratio. However, the relative change brought about by increasing the shear ratio does not appear to be as large as the change in velocity shear; in other words, the increase from $S_r = 1$ to $S_r = 1.5$ is larger than the increase from $S_r = 1.5$ to $S_r = 2$.

Dissipation scaling

The existence of a faster decay rate in the near-field of decaying grid turbulence is typically associated with non-equilibrium turbulence, namely one where the dissipation parameter $C_\varepsilon \equiv \varepsilon L_{11,1}/(\frac{2}{3}k)^{3/2} \neq$ constant. The streamwise variation of the dissipation parameter, for all shear ratios, is shown in fig. 5, which clearly shows that there is a region in the vicinity of the fans where $C_\varepsilon \neq$ constant. For clarity, we have indicated the regions where the two different decay exponents of the turbulent kinetic energy were identified, namely $x < 13M$ and $x \geq 13M$. In the near field, C_ε is found to be increasing at a constant rate, before reaching a transitional zone between $13 \leq x/M \leq 17$, after which it is approximately constant. This transitional region has also been observed in decaying grid turbulence (Valente & Vassilicos, 2011; Hearst & Lavoie, 2016; Nedić & Tavoularis, 2016*b*). The large scatter in C_ε is primarily attributed to the uncertainty in estimating the integral length-scale from the measurements, which was determine by considering 1-second blocks of data and estimating the integral scale from each block. Nevertheless, even with this scatter, the data clearly exhibits a region where $C_\varepsilon \neq$ constant.

It has been observed across a wide range of studies, that $C_\varepsilon \propto \mathrm{Re}_\lambda^{-1}$ (Vassilicos, 2015). A notable exception to this is uniformly sheared turbulence, where scalings of the form $C_\varepsilon \propto \mathrm{Re}_\lambda^{-0.6}$ and $C_\varepsilon \propto \mathrm{Re}_\lambda^{0.5}$ were observed only (Nedić & Tavoularis, 2016*a*). Interestingly, inserting a regular grid into a uniformly sheared flow produced the oft-found scaling of $C_\varepsilon \propto \mathrm{Re}_\lambda^{-1}$ (Nedić & Tavoularis, 2018). The reason for this is still unclear. To facilitate a comparison to other non-equilibrium turbulent shear flows, and in particular to the non-equilibrium

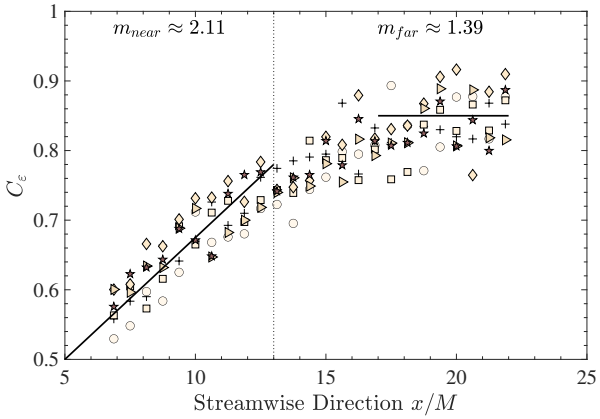

Figure 5. Streamwise variation of the dissipation parameter for different shear ratios.

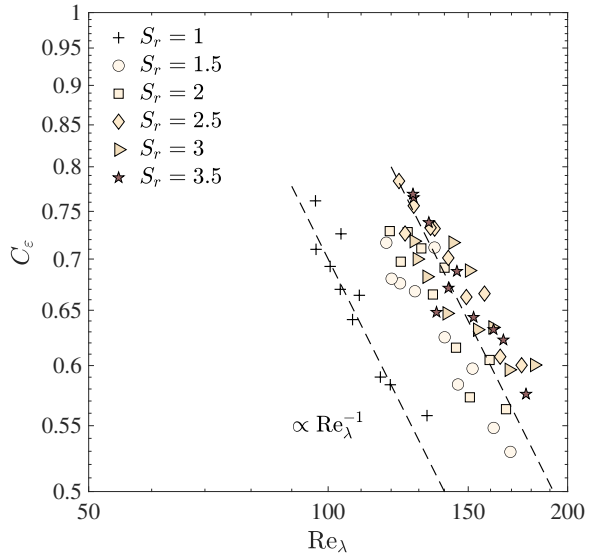

Figure 6. Scaling between the dissipation parameter and the Taylor Reynolds number within the non-equilibrium region.

region of decaying grid-generated turbulence, we examine the scaling between C_ε and Re_λ for this flow. Figure 6 shows this scaling for the non-equilibrium region as identified in fig. 5 i.e., for $x < 13M$ where $m_{near} = 2.11$ and $C_\varepsilon \neq$ constant. We observe a scaling of the form $C_\varepsilon \propto \mathrm{Re}_\lambda^{-1}$ for all shear ratios, which is the same as what has been observed in decaying grid turbulence (Vassilicos, 2015).

CONCLUSIONS

The turbulent flow field downstream of a multi-fan wind tunnel was examined, for a range of shear ratios, at a bulk velocity of $U_\infty = 5$ m/s. By increasing the shear ratio, that being the ratio between the faster and slower velocities produced by the fans, it was possible to increase the turbulent kinetic energy, integral length-scale, and Taylor Reynolds number by as much as 50%. The mean flow was found to be uniform for $x > 13M$, where M is the spacing between the fans. The turbulence field was found to be approximately homogeneous and isotropic at approximately the location where the mean flow became uniform, hence only centreline statistics were considered further. Two distinct regions, based on the decay rate of the kinetic energy, were identified. In a region closer to the fans, namely for $x < 13M$, the decay rate of the turbulent kinetic energy was found to be $m_{near} = 2.11$. For $x \geq 13M$, a slower decay rate of $m_{far} = 1.39$ was observed. The decay rates are similar to those found in decaying grid-generated turbulence, closer to the grid. Examining the dissipation coefficient, it was noted that the region of faster decaying turbulence coincided with the region where the dissipation coefficient increased with streamwise distance, and was hence not-constant. In other words, a non-equilibrium turbulence region exists for $x \geq 13M$, which eventually transitions to an equilibrium region where the decay rate is slower and the dissipation coefficient is constant. Overall, the turbulence generated by the multi-fan wind tunnel was found to exhibit strong similarities, both in terms of nature and scaling, to the near-field of decaying grid-generated turbulence.

REFERENCES

Burattini, Paolo 2008 The effect of the x-wire probe resolution in measurements of isotropic turbulence. *Measurement Science and Technology* **19** (11), 115405.

Comte-Bellot, G & Corrsin, S 1966 The use of a contraction to improve the isotropy of grid-generated turbulence. *Journal of Fluid Mechanics* **25** (4), 657–682.

Hearst, R.J & Lavoie, P 2016 Effects of multi-scale and regular grid geometries on decaying turbulence. *Journal of Fluid Mechanics* **803**, 528–555.

Larssen, J.V & Devenport, W.J 2011 On the generation of large-scale homogeneous turbulence. *Experiments in Fluids* **50** (5), 1207–1223.

Makita, H 1991 Realization of a large-scale turbulence field in a small wind tunnel. *Fluid Dynamics Research* **8** (1-4), 53.

Mydlarski, L 2017 A turbulent quarter century of active grids: from makita (1991) to the present. *Fluid Dynamics Research* **49** (6), 061401.

Nedić, Jovan & Tavoularis, Stavros 2016*a* Energy dissipation scaling in uniformly sheared turbulence. *Physical Review E* **93** (3), 033115.

Nedić, J & Tavoularis, S 2016*b* Measurements of passive scalar diffusion downstream of regular and fractal grids. *Journal of Fluid Mechanics* **800**, 358–386.

Nedić, J & Tavoularis, Stavros 2018 A case study of multi-structure turbulence: Uniformly sheared flow distorted by a grid. *International Journal of Heat and Fluid Flow* **72**, 233–242.

Nishi, A, Kikugawa, H, Matsuda, Y & Tashiro, D 1999 Active control of turbulence for an atmospheric boundary layer model in a wind tunnel. *Journal of Wind Engineering and Industrial Aerodynamics* **83** (1-3), 409–419.

Ozono, S & Ikeda, H 2018 Realization of both high-intensity and large-scale turbulence using a multi-fan wind tunnel. *Experiments in Fluids* **59** (12), 1–12.

Ozono, S, Nishi, A & Miyagi, H 2006 Turbulence generated by a wind tunnel of multi-fan type in uniformly active and quasi-grid modes. *Journal of Wind Engineering and Industrial Aerodynamics* **94** (4), 225–240.

Takamure, K & Ozono, S 2019 Relative importance of initial conditions on outflows from multiple fans. *Physical Review E* **99** (1), 013112.

Valente, P.C. & Vassilicos, J.C. 2011 The decay of turbulence generated by a class of multiscale grids. *Journal of Fluid Mechanics* **687**, 300–340.

Vassilicos, J.C. 2015 Dissipation in turbulent flows. *Annual Review of Fluid Mechanics* **47**, 95–114.